A Spatial-Temporal Decorrelating Receiver for CDMA Systems with Base-Station Antenna Arrays

Ruifeng Wang, *Member, IEEE*, and Steven D. Blostein, *Senior Member, IEEE*

***Abstract*—We investigate multiuser signal detection with a base-station antenna array for a synchronous DS-CDMA uplink using nonorthogonal codes in Rayleigh fading channels. We have developed a new formulation for a spatial-temporal decorrelating detector using the maximum-likelihood criteria. The detector is shown to be near–far resistant. We propose to implement the spatial-temporal decorrelating receiver iteratively by applying the space-alternating generalized expectation-maximization (SAGE) algorithm. Simulation results show that the SAGE-based decorrelating receiver significantly outperforms the conventional single-user receiver and with performance close to that of a spatial-temporal decorrelating receiver with known channel parameters. We have observed that adding base-station antennas can actually improve convergence of the proposed iterative receiver.**

***Index Terms*—Antenna arrays, code-division multiple access, signal detection multiple-access communication.**

I. Introduction

DIRECT-SEQUENCE code-division multiple-access (DS-CDMA) systems use spreading codes to distinguish different mobile users. Because of the relative time delays among the active mobile users, DS-CDMA systems suffer from cochannel interference, which results in the near–far problem [1]. For a synchronous system, the near–far problem is due to the nonorthogonal spreading codes. However, the near–far problem is not inherent to CDMA systems, but due to the conventional single-user receiver which models the interference from other users as noise. By jointly detecting all the users' signals, optimum multiuser signal detection for DS-CDMA systems is near–far resistant and can achieve significant performance improvement over that of conventional single-user detection [2]. Because of the computational complexity of optimum multiuser detection, several suboptimum multiuser signal detectors have been proposed [1], [3]–[5] for additive white Gaussian noise (AWGN) channels. In [6], multiuser signal detection is extended to fading channels. Since multiuser signal detection is near–far resistant, precise power control is not needed.

Paper approved by G. E. Corazza, the Editor for Spread Spectrum of the IEEE Communications Society. Manuscript received December 15, 1998; revised December 24, 2000. This paper was presented in part at the International Conference on Communications (ICC), Vancouver, BC, Canada, 1999.

R. Wang is with Wireless Local Technologies Group, AT&T Wireless Services, Redmond, WA 98073-9759, USA.

S. D. Blostein is with the Department of Electrical and Computer Engineering, Queen's University, Kingston, ON K7L 3N6, Canada (e-mail: sdb@ee.queensu.ca).

This work was supported by the Canadian Institute for Telecommunications Research under the NCE program of the Government of Canada. This paper was presented in part at ICC'99, Vancouver, BC, 1999.

Publisher Item Identifier S 0090-6778(01)01304-6.

Multiple-access interference can also be reduced using array signal processing. By digital beamforming, a base-station antenna array can be used to improve CDMA communication system capacity and coverage (see [7] and references herein). Combined beamformer-RAKE single-user receivers have been proposed for multipath channels in [8] and [9], respectively. In [10], adaptive antenna array processing and interference cancellation approaches using the least mean squared (LMS) algorithm are analyzed and the convergence is found to be very slow, requiring several hundred training bits. The problem of integrating antenna array beamforming and multiuser signal detection is proposed for AWGN channels in [11], but channel estimation has not been addressed.

In order to detect information symbols reliably, we have to estimate channel and antenna array response vectors. Feder and Weinstein apply the expectation-maximization (EM) algorithm to parameter estimation of superimposed signals [12]. Bit sequence detection with joint random parameter estimation using the EM algorithm is studied for single-user systems in [13]. Recently, applications of the EM algorithm to DS-CDMA systems have been proposed for signal detection [14], channel estimation [15] and joint channel estimation, and signal detection [16]. The space-alternating generalized EM (SAGE) algorithm has been developed to accelerate the convergence of the EM algorithm [17]. Applications of the SAGE algorithm in multiuser CDMA channels can be found in [14] for single antenna and known channels, in [18] for antenna array channel parameter estimation, and in [19] for joint parameter estimation and signal detection based on the discrete wavelet transform for a single antenna system.

In this paper, we investigate the integration of spatial signal processing with multiuser signal detection for synchronous DS-CDMA systems with nonorthogonal spreading codes over asynchronous multipath fading channels. We note that that a K-user asynchronous system can be modeled as a synchronous system with $K \times N$ users [1], where N is the number of bits in each transmitted block. The synchronous problem formulation simplifies the derivation and analysis of the new algorithm and the results can be generalized to higher complexity asynchronous multipath systems [20].

This paper is organized as follows. The discrete-time system model is developed in Section II. In Section III, we derive a spatial-temporal decorrelator using the maximum-likelihood criteria and analyze its asymptotic efficiency. An iterative spatial-temporal decorrelating receiver is proposed in Section IV by applying the SAGE algorithm to jointly estimate channel array response vectors and detect information symbol sequences. The bit-error rate (BER) and Cramér–Rao lower

bound (CRLB) for the estimated channel are derived in Section V. Section VI presents simulation results.

II. System Model

To simplify notation, we first consider a synchronous DS-CDMA frequency-nonselective Rayleigh fading uplink channel with a base-station antenna array. We then indicate how to extend the model to asynchronous multipath fading channels.

A. Single-Path Fading Channels

Assuming K active users in the system, an N-bit transmitted signal from the kth user is

$$s_k(t) = A_k \sum_{i=1}^{N} b_k(i) c_k(t - iT_b) \tag{1}$$

where A_k is the amplitude of the kth user, $b_k(i) \in \{-1, 1\}$ is the ith transmitted bit of the kth user with equal probability, $c_k(t)$ represents the spreading waveform of the kth user

$$c_k(t) = \sum_{l=0}^{L-1} c_{kl} p(t - lT_c) \tag{2}$$

$c_{kl} \in \{-1, +1\}$ $(l = 0 \ldots L-1)$ is the spreading code, $p(t)$ is the chip pulse with support T_c, T_c is the chip interval, T_b is the bit interval, and processing gain L is defined as $L = T_b/T_c$. We assume that information bits from K users are independent, the spreading code sequences for K users are independent and the spreading waveform has normalized energy, i.e., $\int_0^{T_b} |c_k(t)|^2 = 1$.

The transmitted signal arrives at a base-station antenna array with M elements. The impulse response of the channel from transmitter to antenna array output can be modeled as

$$\mathbf{g}_k(t) = \alpha_k(t) \mathbf{a}(\theta_k(t)) \delta(t - \tau_k) \tag{3}$$

where $\alpha_k(t)$ represents channel attenuation for user k, $\mathbf{a}(\theta_k(t))$ is the M-dimensional array response vector with direction-of-arrival (DOA) $\theta_k(t)$ from the kth user, and τ_k is the propagation delay between transmitter and receiver for user k. For notational simplicity, we assume $\tau_k = 0$, for $k = 1, \ldots, K$. The channel fading attenuations for K users are assumed to be mutually independent and also independent of information bit symbols.

The received composite signal at the base-station antenna array is

$$\mathbf{x}(t) = \sum_{k=1}^{K} \mathbf{x}_k(t) = \sum_{k=1}^{K} s_k(t) * \mathbf{g}_k(t) + \mathbf{n}(t) \tag{4}$$

where $\mathbf{n}(t)$ is the AWGN vector with zero mean and covariance matrix $\sigma^2 \mathbf{I}_M$, where $\mathbf{I}_M$ is an $M \times M$ identity matrix. Since we assume $\alpha_k(t)$ and $\theta_k(t)$ remain unchanged over the N-bit duration, we drop their time index from here on. From (1) and (2)

$$s_k(t) * \mathbf{g}_k(t) = A_k \alpha_k \mathbf{a}(\theta_k) \sum_{i=1}^{N} b_k(i) c_k(t - iT_b). \tag{5}$$

We denote the channel impulse response vector for user k as $\mathbf{f}_k = A_k \alpha_k \mathbf{a}(\theta_k)$, where the mth component of $\mathbf{f}_k$ is $f_k^m = A_k \alpha_k a^m(\theta_k)$ and $a^m(\theta_k)$ is the mth component of $\mathbf{a}(\theta_k)$. The received signal at the mth array element (for $m = 1, \ldots, M$) is given by

$$x^m(t) = \sum_{k=1}^{K} f_k^m \sum_{i=1}^{N} b_k(i) c_k(t - iT_b) + n^m(t) \tag{6}$$

where $n^m(t)$ is AWGN at the mth array element. The received signal at each element first passes through a filter matched to the chip waveform, and is then sampled at the chip rate. The received discrete-time signal at the ith bit interval from the mth element can be obtained for sample $g \in \{0, 1, \ldots, L-1\}$ as

$$x^m(i, g) = \int_{t = gT_c}^{(g+1)T_c} x^m(t) p^*(t - gT_c)\, dt. \tag{7}$$

Finally, the gth sample of the ith bit for the mth antenna element is obtained in terms of the sampled chips c_{kg} by substituting (6) into (7) yielding

$$x^m(i, g) = \sum_{k=1}^{K} f_k^m c_{kg} b_k(i)/L + n^m(i, g) \tag{8}$$

where $n^m(i, g) = \int_{t=gT_c}^{(g+1)T_c} n^m(t) p^*(t - gT_c)\, dt$ is Gaussian distributed with zero mean and variance σ^2/L. We denote the code vector for the kth user as

$$\mathbf{c}_k = [\, c_{k0}/L \quad c_{k1}/L \quad \cdots \quad c_{k(L-1)}/L \,]^T. \tag{9}$$

The matched filter output at the mth element for $m \in \{1, \ldots, M\}$ can be written in vector form as

$$\mathbf{x}^m(i) = \sum_{k=1}^{K} f_k^m b_k(i) \mathbf{c}_k + \mathbf{n}^m(i) \tag{10}$$

where $\mathbf{n}^m(i) = [n^m(i, 0)\ n^m(i, 1)\ \cdots\ n^m(i, L-1)]^T$.

We define the overall system impulse response vector for user k, including the fading channel, array response vector, and spreading code vector defined above as $\mathbf{h}_k^m = f_k^m \mathbf{c}_k$. Equation (10) can be written as

$$\mathbf{x}^m(i) = \sum_{k=1}^{K} \mathbf{h}_k^m b_k(i) + \mathbf{n}^m(i). \tag{11}$$

Denote $\mathbf{x}(i) = [(\mathbf{x}^1(i))^T \cdots (\mathbf{x}^M(i))^T]^T$, $\mathbf{h}_k = [(\mathbf{h}_k^1)^T \cdots (\mathbf{h}_k^M)^T]^T$, and $\mathbf{n}(i) = [(\mathbf{n}^1(i))^T \cdots (\mathbf{n}^M(i))^T]^T$. The received discrete-time signal from the antenna array is given by

$$\mathbf{x}(i) = \sum_{k=1}^{K} \mathbf{x}_k(i) = \sum_{k=1}^{K} \mathbf{h}_k b_k(i) + \mathbf{n}(i) \tag{12}$$

where $\mathbf{x}_k(i)$ is the received signal from the kth user and $\mathbf{n}(i)$ is AWGN vector with zero mean and covariance matrix $(\sigma^2/L)\mathbf{I}_{ML}$, where $\mathbf{I}_{ML}$ is an $ML \times ML$ identity matrix.

Vector $\mathbf{h}_k$ models the spatial and temporal channel characteristics. The spatial-temporal channel vector $\mathbf{h}_k$ can also be decomposed as

$$\mathbf{h}_k = \begin{bmatrix} \mathbf{c}_k & \mathbf{0} & \cdots & \mathbf{0} \\ \mathbf{0} & \mathbf{c}_k & \ddots & \mathbf{0} \\ \vdots & \ddots & \ddots & \vdots \\ \mathbf{0} & \mathbf{0} & \cdots & \mathbf{c}_k \end{bmatrix} \begin{bmatrix} f_k^1 \\ f_k^2 \\ \vdots \\ f_k^M \end{bmatrix} = C_k \mathbf{f}_k \tag{13}$$

where C_k is an $ML \times M$ spreading code sequence matrix of the kth user.

Denote matrix $\mathcal{H} = [\mathbf{h}_1 \vdots \cdots \vdots \mathbf{h}_K]$ and vector $\mathbf{b}(i) = [b_1(i) \ \cdots \ b_K(i)]^T$, (12) can be expressed as

$$\mathbf{x}(i) = \mathcal{H}\mathbf{b}(i) + \mathbf{n}(i). \tag{14}$$

A necessary condition that K users are identifiable is that $\mathcal{H}$ be of full column rank, implying that $ML > K$.

B. Asynchronous Multipath Fading Channels

Using the synchronous-equivalent model described in [21], the above formulation may be extended to the case of P resolvable signal paths per user, each with delay $\tau_{k,p} \in [0, T_b)$ for $k \in \{1, \ldots K\}$ and $p \in \{1, \ldots P\}$. All paths corresponding to one bit from a user are assumed be contained in a $2T_b$ interval, and therefore three consecutive bit intervals are required for each user [21]. We denote a $3K$-dimensional vector centered at bit i by $\mathbf{b}_k^w(i) = [b_k(i-1) \ b_k(i) \ b_k(i+1)]^T$. Let $H_k = \sum_{p=1}^{P} H_{k,p}$ denote the channel response for user k, where $H_{k,p}$ is the response to path p. The $2ML$-element received signal vector is then

$$\mathbf{x}(i) = \sum_{k=1}^{K} H_k \mathbf{b}_k^w(i) + \mathbf{n}(i). \tag{15}$$

We denote $2ML \times 3K$ channel matrix $\mathcal{H} = [H_1 \vdots \cdots \vdots H_K]$ and $\mathbf{b}^w(i) = [\mathbf{b}_1^w(i)^T \ \cdots \ \mathbf{b}_K^w(i)^T]^T$. The synchronous equivalent discrete-time model is given by

$$\mathbf{x}(i) = \mathcal{H}\mathbf{b}^w(i) + \mathbf{n}(i). \tag{16}$$

Adding path subscripts p to (13), we obtain for $n \in \{-1, 0, 1\}$

$$\begin{bmatrix} f_{k,p}^1 \mathbf{c}_{k,p}^n \\ \vdots \\ f_{k,p}^M \mathbf{c}_{k,p}^n \end{bmatrix} = \begin{bmatrix} \mathbf{c}_{k,p}^n & \cdots & \mathbf{0} \\ \vdots & \ddots & \vdots \\ \mathbf{0} & \cdots & \mathbf{c}_{k,p}^n \end{bmatrix} \begin{bmatrix} f_{k,p}^1 \\ \vdots \\ f_{k,p}^M \end{bmatrix} \equiv C_{k,p}^n \mathbf{f}_{k,p} \tag{17}$$

and

$$H_{k,p} = \begin{bmatrix} C_{k,p}^{-1} & \vdots & C_{k,p}^0 & \vdots & C_{k,p}^1 \end{bmatrix} \begin{bmatrix} \mathbf{f}_{k,p} & \mathbf{0} & \mathbf{0} \\ \mathbf{0} & \mathbf{f}_{k,p} & \mathbf{0} \\ \mathbf{0} & \mathbf{0} & \mathbf{f}_{k,p} \end{bmatrix} \equiv C_{k,p} F_{k,p}. \tag{18}$$

The spatial-temporal channel matrix for the kth user can be expressed as

$$H_k = \sum_{p=1}^{P} C_{k,p} F_{k,p} \tag{19}$$

where $3M \times 3$ matrix $F_{k,p}$ represents the spatial array channel impulse response in multipath fading and $2ML \times 3M$ matrix $C_{k,p}$ represents the temporal channel impulse response, incorporating spreading code and path delay.

III. Spatial-Temporal Decorrelator

For the single-path case, the log-likelihood of the received signal $\mathbf{x}(i)$ conditioned on the bit vector $\mathbf{b}(i)$ and the spatial-temporal channel matrix $\mathcal{H}$ is given by (omitting index i)

$$\Omega(\mathbf{b}, \mathcal{H}) = -\frac{1}{\sigma^2/L}(\mathbf{x} - \mathcal{H}\mathbf{b})^H(\mathbf{x} - \mathcal{H}\mathbf{b}) \tag{20}$$

where superscript H denotes conjugate transpose. The unknown parameters are $\mathbf{b}$ and $\mathcal{H}$. If $\mathcal{H}$ is available, the bit vector decision variable $\hat{\mathbf{b}}$ can be obtained by maximizing (20)

$$\hat{\mathbf{b}}_d = \arg\max_{\mathbf{b}} \Omega(\mathbf{b}, \mathcal{H}). \tag{21}$$

Equating the derivative of (20) with respect to $\mathbf{b}$ to zero, we obtain

$$\hat{\mathbf{b}} = \text{sign}\{[\mathcal{H}^H\mathcal{H}]^{-1}\mathcal{H}^H\mathbf{x}\} \tag{22}$$

where $\text{sign}\{a\} = 1$ if $a \geq 0$ or -1 if $a < 0$.

We define the spatial-temporal cross-correlation matrix as

$$R = \mathcal{H}^H\mathcal{H} = [C_1\mathbf{f}_1 \quad C_2\mathbf{f}_2 \quad \cdots \quad C_K\mathbf{f}_K]^H \times [C_1\mathbf{f}_1 \quad C_2\mathbf{f}_2 \quad \cdots \quad C_K\mathbf{f}_K]. \tag{23}$$

Denoting $f_{ij} = \mathbf{f}_i^H\mathbf{f}_j$ and

$$\rho_{ij} = \mathbf{c}_i^H\mathbf{c}_j \begin{cases} \leq 1/L, & \text{if } i \neq j \\ = 1/L, & \text{if } i = j \end{cases} \tag{24}$$

if the spreading codes are orthogonal, $\rho_{ij} = \mathbf{c}_i^H\mathbf{c}_j = 0$ (for $i \neq j$) for a synchronous system. We consider the case where the system is asynchronous and/or the spreading codes are not orthogonal and we cannot guarantee zero cross correlation. Using (23) and (24), R is given by

$$R = \begin{bmatrix} f_{11}\rho_{11} & f_{12}\rho_{12} & \cdots & f_{1K}\rho_{1K} \\ f_{21}\rho_{21} & f_{22}\rho_{22} & \cdots & f_{2K}\rho_{2K} \\ \vdots & \ddots & \ddots & \vdots \\ f_{K1}\rho_{K1} & f_{K2}\rho_{K2} & \cdots & f_{KK}\rho_{KK} \end{bmatrix}. \tag{25}$$

We may interpret (22) as follows. Let

$$\mathbf{z} = \mathcal{H}^H\mathbf{x} = \begin{bmatrix} \mathbf{f}_1^H & \mathbf{0}^T & \cdots & \mathbf{0}^T \\ \mathbf{0}^T & \mathbf{f}_2^H & \ddots & \mathbf{0}^T \\ \vdots & \ddots & \ddots & \vdots \\ \mathbf{0}^T & \mathbf{0}^T & \cdots & \mathbf{f}_K^H \end{bmatrix} \begin{bmatrix} \mathbf{y}_1 \\ \mathbf{y}_2 \\ \vdots \\ \mathbf{y}_K \end{bmatrix} = F^H\mathbf{y} \tag{26}$$

using (13) where $\mathbf{y}_k = C_k^H\mathbf{x}$ for $k = 1, 2, \ldots, K$. Thus, $\mathbf{y}_k$ actually represents the despread output for the kth user's deci-

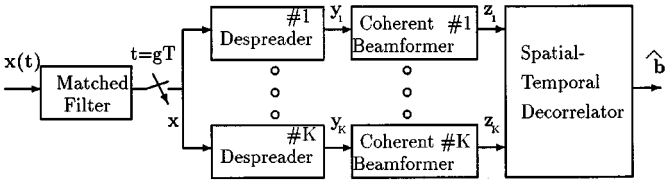

Fig. 1. Spatial-temporal decorrelator structure.

sion variable. The detector structure implied by (26) is a conventional single-user detector with maximum signal-to-noise ratio (SNR) beamforming, which we refer to simply as the conventional single-user detector. Using (22), (25), and (26), the detected bit vector can be written in the form

$$\hat{\mathbf{b}} = \text{sign}\{R^{-1}F^H\mathbf{y}\}. \tag{27}$$

Therefore, the final data decision vector is obtained by decorrelating the conventional single-user detector output. Equation (27) can also be viewed as maximum signal-to-interference-plus-noise ratio beamforming. Matrix R includes both temporal cross correlation due to nonorthogonal spreading codes and spatial correlation arising from the spatial distribution of active users. The detector structure, illustrated in Fig. 1, differs from that of [11] since the matched-filter (despreader) occurs prior to beamforming. For known channels, the difference in structure may not be significant. However, for unknown channels, Fig. 1 has the practical advantage over that in [11] since an estimate of the channel array response required for beamforming can be computed from the despread output.

Substituting (14) into (22) and using definition of R [cf. (23)], the spatial-temporal decorrelator output can be simplified to

$$\hat{\mathbf{b}} = \text{sign}\{\mathbf{b} + R^{-1}\mathbf{n}_d\} = \text{sign}\{\mathbf{b} + \mathbf{w}\} \tag{28}$$

where $\mathbf{w}$ is the spatial-temporal decorrelator output AWGN vector with zero mean and covariance matrix $(\sigma^2/L)R^{-1}$. If there is no base-station antenna array, the spatial-temporal detector reduces to the classical decorrelating detector proposed in [1]. A similar development can be obtained for the multipath case, with the added step of maximal-ratio path combining of beamformer outputs. We have omitted the details.

A. Near–Far Resistance

The asymptotic efficiency is a performance measure for multiuser signal detection in the limit as the background noise goes to zero. The kth user's asymptotic efficiency is defined as [2]

$$\eta_k = \lim_{\sigma\to 0}\frac{e_k(\sigma)}{w_k} = \sup\left\{0 \le r \le 1 : \lim_{\sigma\to 0}\frac{P_k(\sigma)}{Q\left(\frac{\sqrt{rw_k}}{\sigma}\right)} < +\infty\right\} \tag{29}$$

where $e_k(\sigma)$ is the kth user's effective energy required to achieve the same error probability in the absence of interferers, w_k is the received energy for user k, $P_k(\sigma)$ represents BER of the kth user when the variance of AWGN is σ^2, and $Q(x) = \int_x^\infty(\exp(-y^2/2)/\sqrt{2\pi})\,dy$.

Because the asymptotic efficiency of the temporal decorrelator in a single-path Rayleigh fading channel is the same as that of an AWGN channel [6], we only need to consider the AWGN channel here. In this case, $\mathbf{f}_k = A_k\mathbf{a}_k(\theta_k)$.

The kth user's bit-error probability for the spatial-temporal decorrelator can be obtained as

$$P_k^d = Q\left(\frac{1}{\frac{\sigma}{\sqrt{L}}\sqrt{(R^{-1})_{kk}}}\right) \tag{30}$$

where $(R^{-1})_{kk}$ represents the kth diagonal element of matrix R^{-1} [3]. Thus, the asymptotic efficiency of the spatial-temporal decorrelator for the kth user is given by

$$\eta_k^d = \max^2\left\{0, \frac{1}{\sqrt{R_{kk}(R^{-1})_{kk}}}\right\} = \frac{1}{R_{kk}(R^{-1})_{kk}}. \tag{31}$$

By formulating the bit-error probability for the conventional single-user detector and identifying the dominating term when the background noise tends to zero [22], the kth user's asymptotic efficiency of the conventional single-user detector can be obtained

$$\eta_k^c = \max^2\left\{0, \frac{\sqrt{R_{kk}} - \sum_{i\neq k}|R_{ik}|/\sqrt{R_{kk}}}{\sqrt{R_{kk}}}\right\} = \max^2\left\{0, 1 - \sum_{i\neq k}\frac{|R_{ik}|}{R_{kk}}\right\}. \tag{32}$$

The kth user's near–far resistance is defined as its worst-case asymptotic efficiency over all possible energies of the interferers and given by $\bar{\eta}_k = \inf_{w_i\ge 0, i\neq k}\eta_k$ [1]. An analogous expression can be obtained for the asynchronous multipath case using the synchronous-equivalent model described earlier.

Example 1: To compare the asymptotic efficiency for the spatial-temporal decorrelator and the conventional single-user detector, we consider a four-user system based on length-7 Gold codes as spreading sequences. The corresponding cross-correlation matrix of the spreading codes is in [5]. We assume a uniform linear array (ULA) with half-wavelength spacing at the base-station. The DOAs for four active users with known array responses are $[25°, 5°, -15°, -35°]$ with respect to the array boresight. We consider a single antenna as well as a three-element array. We assume that all interferers have equal transmitted power. We refer to user 1 as the desired user and define the power ratios A_k^2/A_1^2, for $k = 2, \ldots, K$. Fig. 2 depicts spatial-temporal decorrelator performance independent of the received interference energy, i.e., near–far resistance. The asymptotic efficiencies for conventional single-user detectors with or without an array tends to zero as the interferers become stronger. However, the antenna array is able to improve asymptotic efficiency for either the decorrelating or conventional single-user detectors.

The above analysis is based on the assumption that R is known, implying that array response vectors, $\mathbf{f}_k$ (for $k = 1, 2, \ldots, K$), are known at the receiver. Since this is not the case in practice, we now investigate joint channel estimation and signal detection.

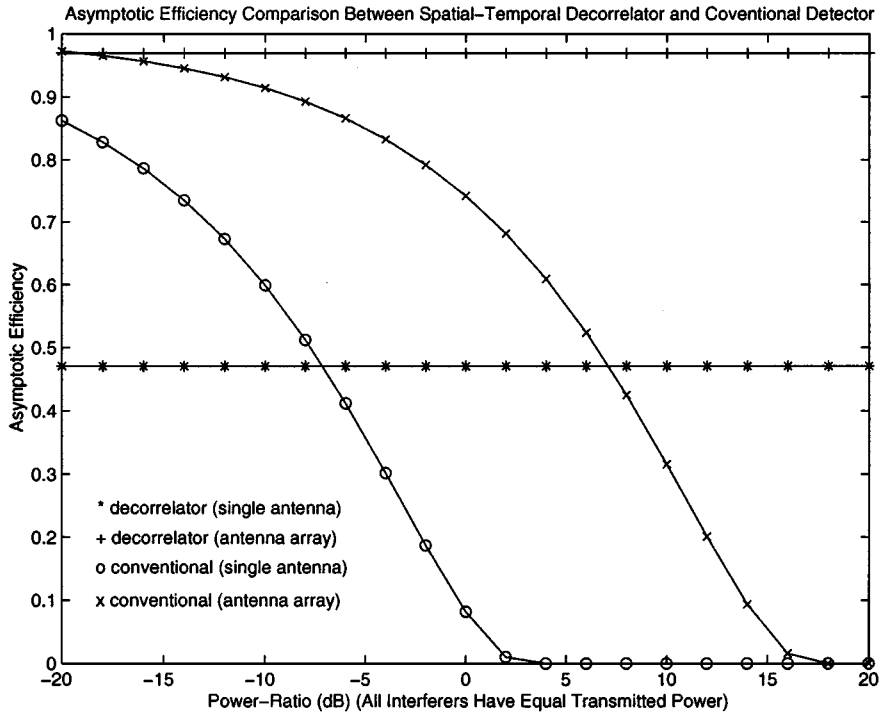

Fig. 2. Asymptotic efficiencies for single antenna and a three-element antenna array.

IV. Decorrelating Receiver via SAGE Algorithm

In this section, we address the key implementation issue of the proposed spatial-temporal decorrelating receiver, namely the joint parameter estimation and spatial-temporal signal decorrelation. Again, we omit the details for the multipath case for the sake of clarity. We derive a sequential decision-feedback receiver structure based on the SAGE algorithm. The available observed data at the receiver is a data vector set $\{\mathbf{x}(i); 1, \ldots, N\}$.

The SAGE algorithm can achieve improved performance, such as faster convergence, over the standard EM algorithm [17]. The key idea for the SAGE algorithm is to choose a less informative hidden-data space to improve convergence rate.

Starting with an initial parameter vector estimate at iteration $j = 0$, iterate the following steps.

1) Choose a new index set $S = S^j$, a subset of the parameters, which defines an admissible hidden-data space $\mathbf{x}^{S^j}$.
2) Compute the following conditional expectation of $\mathbf{x}^{S^j}$ given observed data $\mathbf{x}$ and the previous estimate of parameter vector $\hat{\theta}^j$

$$\Omega(\theta_{S^{j+1}} \,|\, \hat{\theta}^j) = E[\ln f(\mathbf{x}_{S^j} \,|\, \mathbf{x}_{S^j}, \hat{\theta}_{\bar{S}^j}) \,|\, \mathbf{x}, \hat{\theta}^j]. \tag{33}$$

3) Obtain the next estimate by maximizing over the chosen subset while keeping the other parameters fixed

$$\begin{aligned} \hat{\theta}^{j+1}_{S^{j+1}} &= \arg\max_{\theta_{S^{j+1}}} \Omega(\theta_{S^{j+1}} \,|\, \hat{\theta}^j) \\ \hat{\theta}^{j+1}_{\bar{S}^{j+1}} &= \hat{\theta}^j_{\bar{S}^{j+1}} \end{aligned} \tag{34}$$

where the index set $\bar{S}^j$ is the complement of S^j.

4) Increment j and go to step 1.

A. Application to CDMA

For the case of our DS-CDMA system model, we would like to estimate each user's channel parameters and detect information symbols individually. In step 1, we choose user index k as the index set. Thus, the admissible hidden-data space for index k, for $k = 1, \ldots, K$ and $i = 1, \ldots, N$, is given by (12)

$$\mathbf{x}_k^S(i) \sim \mathbf{N}\left(\mathbf{h}_k b_k(i), \frac{\sigma^2}{L}\mathbf{I}_{ML}\right). \tag{35}$$

The log-likelihood function after removing the terms independent of $\mathbf{h}_k$ and $b_k(i)$ is straightforward

$$\begin{aligned} &\Omega\left(\mathbf{x}_k^S(1), \ldots, \mathbf{x}_k^S(N)\right) \\ &\quad = -\frac{1}{\sigma^2/L}\sum_{i=1}^{N}\left(\mathbf{x}_k^S(i) - \mathbf{h}_k b_k(i)\right)^H\left(\mathbf{x}_k^S(i) - \mathbf{h}_k b_k(i)\right). \end{aligned} \tag{36}$$

Given the estimation results at the jth iteration, the conditional expectation of $\mathbf{x}_k^S(i)$ (for $k = 1, \ldots, K$ and $i = 1, \ldots, N$) in step 2 is given by

$$\begin{aligned} \hat{\mathbf{x}}_k^S(i) &= \hat{\mathbf{h}}_k^j \hat{b}_k^j(i) + \left(\mathbf{x}(i) - \sum_{k=1}^{K}\hat{\mathbf{h}}_k^j \hat{b}_k^j(i)\right) \\ &= \mathbf{x}(i) - \sum_{k_1 \neq k}\hat{\mathbf{h}}_{k_1}^j \hat{b}_{k_1}^j(i). \end{aligned} \tag{37}$$

Finally, substituting (37) into (36), we obtain the conditional expectation of the log-likelihood function of $\mathbf{x}_k^S(i)$. The maximization result at the next iteration, (34) in step 3, is given by

$$\begin{aligned} \left[\hat{\mathbf{h}}_k^{j+1}, \hat{b}_k^{j+1}(i)\right] = \arg\max_{\mathbf{h}_k, b_k(i)} &-\sum_{i=1}^{N}\left(\hat{\mathbf{x}}_k^S(i) - \mathbf{h}_k b_k(i)\right)^H \\ &\times \left(\hat{\mathbf{x}}_k^S(i) - \mathbf{h}_k b_k(i)\right). \end{aligned} \tag{38}$$

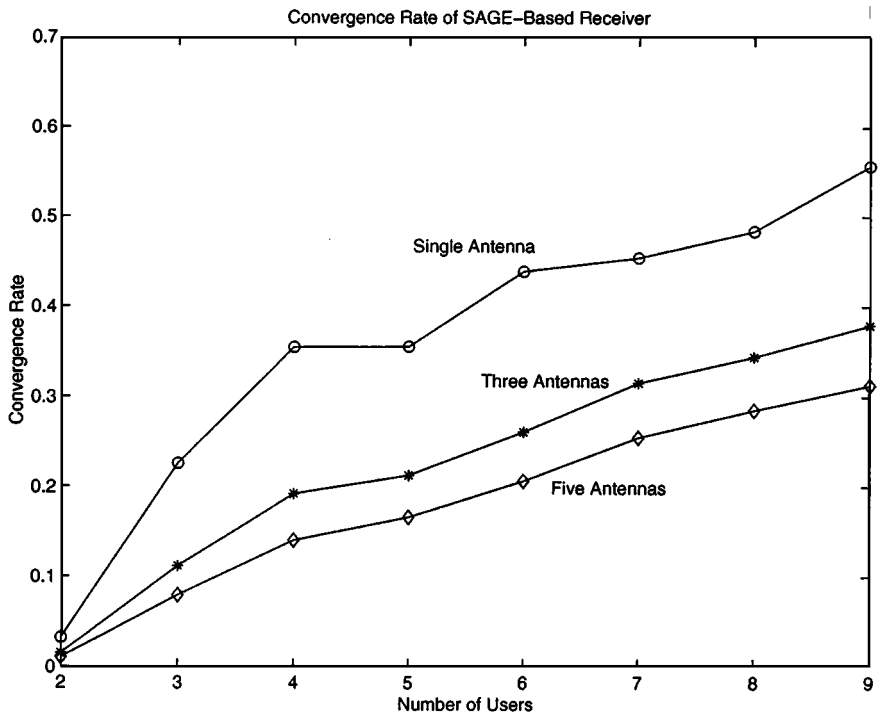

Fig. 3. Convergence rate of SAGE-based receiver. (A larger rate implies slower convergence. The algorithm converges faster as the number of antennas increases.)

Thus, the SAGE-based receiver for joint array response vector estimation and information symbol detection can be summarized by the following steps.

1) Initialize iteration $j = 0$.
2) Choose new index set: $k = (j \bmod K)$.
3) E-step: (conditional expectation of hidden-data)
   For $i = 1, \ldots, N$

$$\hat{\mathbf{x}}_k^{S^{j+1}}(i) = \mathbf{x}(i) - \sum_{k_1=1, \neq k}^{K} \hat{\mathbf{h}}_{k_1}^j \hat{b}_{k_1}^j(i). \tag{39}$$

4) M-step: (maximum-likelihood estimation)

$$\hat{\mathbf{h}}_k^{j+1} = \frac{1}{N} \sum_{i=1}^{N} \hat{\mathbf{x}}_k^{S^{j+1}}(i) \hat{b}_k^j(i) \tag{40}$$

$$\hat{b}_k^{j+1}(i) = \operatorname{sign}\left\{ \left(\hat{\mathbf{h}}_k^{j+1} \right)^H \hat{\mathbf{x}}_k^{S^{j+1}}(i) \right\} \tag{41}$$

$$\hat{\mathbf{h}}_{k'}^{j+1} = \hat{\mathbf{h}}_{k'}^j, \qquad k' \neq k$$
$$\hat{b}_{k'}^{j+1}(i) = \hat{b}_{k'}^j(i), \qquad k' \neq k.$$

5) Increment j and go to step 2.

The above steps can be interpreted as follows. Substituting (39) into (41), we obtain

$$\hat{b}_k^{j+1}(i) = \operatorname{sign}\left\{ \left(\left(\hat{\mathbf{h}}_k^{j+1} \right)^H \mathbf{x}_k(i) - \sum_{k'=1, k' \neq k}^{K} \hat{f}_{kk'}^{j+1} \rho_{kk'} \hat{b}_k^j(i) \right) \right\} \tag{42}$$

where $\hat{f}_{kk'}^{j+1} = (\hat{\mathbf{f}}_k^{j+1})^H \hat{\mathbf{f}}_{k'}^j$ is the estimated instantaneous spatial correlation at the $(j+1)$th iteration and $\rho_{kk'}$ is the cross correlation defined in (24). Equation (42) implies that information bit detection at each iteration involves explicit interference cancellation given current channel estimates and previously detected bits. Therefore, the SAGE-based receiver has a sequential interference cancellation structure. The initial guesses for the channel estimates are obtained using the conventional receiver with a pilot bit for each user.

B. Convergence

From (20), it can be verified that the log-likelihood function is continuous and differentiable with respect to the unknown parameters. Since the likelihood function increases monotonically with each iteration and is bounded above, the proposed receiver converges to a fixed stationary point or local/global maxima depending on the initial guess of the unknown parameters [23]. The convergence rate of the SAGE-based receiver can be shown to be the largest eigenvalue of $[F_{\mathbf{x}_k^S} - F_{\mathbf{x}}](F_{\mathbf{x}_k^S})^{-1}$ [24], where $F_{\mathbf{x}_k^S}$ and $F_{\mathbf{x}}$ are Fisher information matrices of $\mathbf{x}_k^S$ and $\mathbf{x}$, respectively. To investigate the effect of an antenna array on receiver convergence, we assume, for simplicity, that the channel array response vectors are known. From (20) and (37), $F_{\mathbf{x}} = (4L/\sigma^2)R$ and $F_{\mathbf{x}_k^S} = (4L/\sigma^2)R_{kk}\mathbf{I}_K$. Thus, the convergence rate of the SAGE-based receiver is given by $\mu = \text{maxeigenvalue}\{\mathbf{I}_k - R_{kk}^{-1}R\}$.

Example 2: We again consider a basestation with a half-wavelength-spaced ULA in an AWGN channel. The DOAs of active users are uniformly distributed in $[-60°, 60°]$. Gold sequences of length-31 from [25] are assigned to mobile users. All active users have equal transmitted power. The convergence rate curves are plotted in terms of number of users and number of antennas and averaged over 5000 trials. From Fig. 3, we observe slower convergence with an increasing number of active users. However, using an antenna array with high inter-element correlation improves receiver convergence due to added redundant

channel information. Channel estimation performance improvements using antenna arrays is further documented in Section VI.

V. Receiver Performance

To assess the performance of the proposed spatial-temporal decorrelating receiver, we determine the BER for symbol detection and the CRLB for channel estimation.

A. BER

For the single-path case, it is observed from (28) that the bit decision vector is an unbiased estimator with zero-mean noise vector $\mathbf{w}$ and covariance matrix $(\sigma^2/L)R^{-1}$. We assume that the channels are perfectly known. The BER analysis in this section is compared to simulations of the SAGE-based receiver with imperfect channel estimates.

Claim: Without loss of generality, the BER for user 1 is given by

$$P_1 = \frac{1}{2}\left(1 - \sqrt{\frac{\bar{\gamma}_1}{1+\bar{\gamma}_1}}\right) \tag{43}$$

where $\bar{\gamma}_1$ is the average SNR for user 1 and given by

$$\bar{\gamma}_1 = \frac{1}{\frac{\sigma^2}{L}E[R^{-1}]_{11}} \tag{44}$$

and

$$E[R^{-1}]_{11} = \frac{1}{\mathrm{Var}[\alpha_1]} \frac{\begin{vmatrix} \xi_{22} & \cdots & \xi_{2K} \\ \vdots & \ddots & \vdots \\ \xi_{K2} & \cdots & \xi_{KK} \end{vmatrix}}{\begin{vmatrix} \xi_{11} & \cdots & \xi_{1K} \\ \vdots & \ddots & \vdots \\ \xi_{K1} & \cdots & \xi_{KK} \end{vmatrix}} \tag{45}$$

where $E[\cdot]$ denotes expectation over Rayleigh random variables contained in R^{-1}, $\mathrm{Var}[\cdot]$ represents variance, $|\cdot|$ is the determinant, and $\xi_{ij} = A_i A_j \mathbf{a}_i^H \mathbf{a}_j \rho_{ij}$.

Proof: The (1, 1) entry of R^{-1} is

$$[R^{-1}]_{11} = \frac{1}{|R|}\begin{vmatrix} R_{22} & \cdots & R_{2K} \\ \vdots & \ddots & \vdots \\ R_{K2} & \cdots & R_{KK} \end{vmatrix}.$$

Since the ijth entry of R is given by $R_{ij} = \alpha_i^* \alpha_j \xi_{ij}$, using Hermitian symmetry, it can be easily obtained that

$$\begin{vmatrix} R_{22} & \cdots & R_{2K} \\ \vdots & \ddots & \vdots \\ R_{K2} & \cdots & R_{KK} \end{vmatrix} = |\alpha_2|^2 \ldots |\alpha_K|^2 \begin{vmatrix} \xi_{22} & \cdots & \xi_{2K} \\ \vdots & \ddots & \vdots \\ \xi_{K2} & \cdots & \xi_{KK} \end{vmatrix} \tag{46}$$

and

$$|R| = |\alpha_1|^2 \ldots |\alpha_K|^2 \begin{vmatrix} \xi_{11} & \cdots & \xi_{1K} \\ \vdots & \ddots & \vdots \\ \xi_{K1} & \cdots & \xi_{KK} \end{vmatrix} \tag{47}$$

where $|\alpha_k|^2 = \alpha_k^* \alpha_k$, from which (45) follows. For Rayleigh fading and binary phase-shift keying modulation, (43) is obtained using the results in [26]. ■

For the case of multipath channels, we instead bound the BER assuming that all multiple-access interference is cancelled at the last SAGE iteration, and that all channel array response vectors are perfectly known. In addition, we approximate the covariance matrix $\mathcal{R}$ as diagonal, which we have verified to be reasonably accurate [28]. After these steps have been carried out, the BER lower bound for the kth user can be obtained using [26, p. 781]

$$P_k = [(1-\mu)/2]^P \sum_{p=0}^{P-1} \binom{P-1+p}{p} [(1+\mu)/2]^p \tag{48}$$

where $\mu = \sqrt{\bar{\gamma}_c/(1+\bar{\gamma}_c)}$ and $\bar{\gamma}_c = (MLA_k^2 \rho_{kk,11}^{0,0}/\sigma^2)$ $E[\alpha_{k,p}^2]$. The $\alpha_{k,p}$ denotes the attenuation of the pth path of user k, and the temporal correlation coefficient $\rho_{kk,11}^{0,0} = \mathbf{c}_{k,1}^{0H}\mathbf{c}_{k,1}^0$. It has been assumed that $\rho_{kk,pp}^{0,0}$ are identically distributed for all $p \in \{1, \ldots P\}$.

B. CRLB

To measure channel array response vector estimation performance, we derive the CRLB. We collect the unknown parameters into column vector $\mathbf{a} = [\mathbf{a}_1^T \ \cdots \ \mathbf{a}_K^T]^T$, where $\mathbf{a}_k = \alpha_k \mathbf{a}(\theta_k)$ is the channel array response vector for the kth user.

For an M-element antenna array, we define the $M \times M$ matrix for the ith bit of the kth user, $k = 1, \ldots, K$, as $B_k(i) = \mathrm{diag}[b_k(i), \ldots, b_k(i)]$.

Proposition: The CRLB matrix for parameter vector $\mathbf{a}$ is given by

$$\mathbf{CRLB}(\mathbf{a}) = \frac{1}{L}\left[\sum_{i=1}^{N} G(i)\right]^{-1} \tag{49}$$

where

$$G(i) = \begin{bmatrix} \gamma_1 \rho_{11} I_M & \cdots & \sqrt{\gamma_1 \gamma_K}\rho_{1K}\mathbf{B}_{1K}(i) \\ \sqrt{\gamma_1\gamma_2}\rho_{12}\mathbf{B}_{12}(i) & \ddots & \vdots \\ \vdots & \ddots & \vdots \\ \sqrt{\gamma_1\gamma_K}\rho_{1K}\mathbf{B}_{1K}(i) & \cdots & \gamma_K \rho_{KK} I_M \end{bmatrix} \tag{50}$$

where $\mathbf{B}_{kj}(i) = B_k^H(i)B_j(i) = \mathbf{I}_M$ if $b_k(i) = b_j(i)$ or $-\mathbf{I}_M$ if $b_k(i) = -b_j(i)$ (for $i = 1, \ldots, N$ and $k, j = 1, \ldots, K$), $\gamma_k = A_k^2/\sigma^2$ is the SNR corresponding to the kth user and ρ_{ij} is the spreading code cross correlation defined in (24).

Outline of Proof: First, we define the parameter vector as $\phi = [\sigma^2 \ \bar{\mathbf{a}}^T \ \check{\mathbf{a}}^T]^T$, where σ^2 is background noise covariance, $\bar{\mathbf{a}}$ and $\check{\mathbf{a}}$ are the real and imaginary parts of $\mathbf{a}$, respectively. Discarding the terms independent of ϕ, the log-likelihood function is given by

$$\ln \Omega = -MLN \ln \sigma^2 - \frac{L}{\sigma^2}\sum_{i=1}^{N}[\mathbf{x}(i) - \mathcal{H}\mathbf{b}(i)]^H[\mathbf{x}(i) - \mathcal{H}\mathbf{b}(i)]). \tag{51}$$

We compute the derivative of (51) with respect to ϕ. Using the definition of the Fisher information matrix

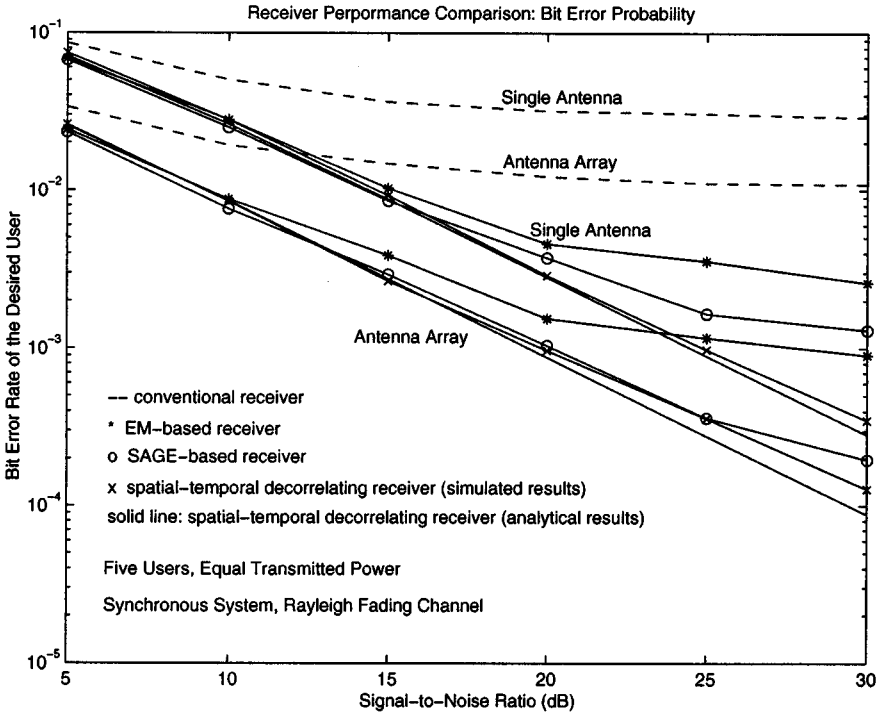

Fig. 4. BER for single antenna and a three-element antenna array.

$\mathbf{I}(\phi) = E[(\partial \ln \Omega/\partial\phi)(\partial \ln \Omega/\partial\phi)^T]$ and following the technique in [27], we obtain

$$\mathbf{I}(\bar{\mathbf{a}}) = E\left[\left(\frac{\partial \ln \Omega}{\partial \bar{\mathbf{a}}}\right)\left(\frac{\partial \ln \Omega}{\partial \bar{\mathbf{a}}}\right)^T\right] = \frac{2L}{\sigma^2}\sum_{i=1}^{N} \mathrm{Re}[B^H(i)D^H DB(i)]$$

$$\mathbf{I}(\check{\mathbf{a}}) = E\left[\left(\frac{\partial \ln \Omega}{\partial \check{\mathbf{a}}}\right)\left(\frac{\partial \ln \Omega}{\partial \check{\mathbf{a}}}\right)^T\right] = \frac{2L}{\sigma^2}\sum_{i=1}^{N} \mathrm{Re}[B^H(i)D^H DB(i)]$$

$$\mathbf{I}(\bar{\mathbf{a}}\check{\mathbf{a}}) = E\left[\left(\frac{\partial \ln \Omega}{\partial \bar{\mathbf{a}}}\right)\left(\frac{\partial \ln \Omega}{\partial \check{\mathbf{a}}}\right)^T\right] = -\frac{2L}{\sigma^2}\sum_{i=1}^{N} \mathrm{Im}[B^H(i)D^H DB(i)]$$

where $B(i) = \mathrm{diag}[B_1(i), \ldots, B_K(i)]$ and $D = [D_1 \vdots \cdots \vdots D_K]$ with $ML \times M$ matrix $D_k = \mathrm{diag}[A_k\mathbf{c}_k, \ldots, A_k\mathbf{c}_k]$ (for $k = 1, \ldots, K$). Defining $G(i) = (1/\sigma^2)B^H(i)D^H DB(i)$, (50) follows. Since $G(i)$ (for $i = 1, \ldots, N$) is real, we have $\mathbf{I}(\bar{\mathbf{a}}\check{\mathbf{a}}) = \mathbf{0}$ and

$$\mathbf{I}(\bar{\mathbf{a}}) = \mathbf{I}(\check{\mathbf{a}}) = 2L\sum_{i=1}^{N} G(i). \tag{52}$$

Thus, the Fisher information matrix is given by

$$\mathbf{I}(\phi) = \begin{bmatrix} \mathbf{I}(\sigma^2) & \mathbf{0}_{MK}^T & \mathbf{0}_{MK}^T \\ \mathbf{0}_{MK} & \mathbf{I}(\bar{\mathbf{a}}) & \mathbf{0} \\ \mathbf{0}_{MK} & \mathbf{0} & \mathbf{I}(\check{\mathbf{a}}) \end{bmatrix}. \tag{53}$$

Finally, using inverse of a partitioned matrix, we can obtain the CRLB matrix for channel array response vectors $\mathbf{CRLB}(\mathbf{a}) = \mathbf{I}(\bar{\mathbf{a}})^{-1} + \mathbf{I}(\check{\mathbf{a}})^{-1}$. ■

Clearly, the Fisher information matrix, $\sum_{i=1}^{N} G(i)$, is a function of the SNR at the ith bit as well as the cross correlation between the spreading codes.

VI. Simulations

Randomly generated length-31 Gold sequences are assigned to CDMA users. We transmit a 100-bit information sequence from each user and assume the channels remain unchanged. We insert one training bit in the first bit position in each sequence to obtain initial guesses for the channel array response vectors. A ULA with $\lambda/2$ spacing is used at the base-station and the DOAs are uniformly distributed in $[-60°, 60°]$. We assume that the channels are Rayleigh-fading and that the reported SNR value is averaged over the fading. Therefore, the required SNR to achieve a target BER is higher than that for AWGN channels. Using (26), we obtain the initial detected bit vectors. We assume that the first user is the desired user in all simulations. The results are computed from 10 000–150 000 trials, depending on the SNR, so that the BER is calculated to within ±5% with 90% confidence.

First, we compare performances of the SAGE-based, EM-based [16], and spatial-temporal decorrelating receiver with perfect channel array response knowledge. There are five active users in the system and either a single antenna or a three-element base-station antenna array. For simplicity, all users have equal transmitted power. Both the SAGE and EM-based decorrelating receivers use eight iterations. From Fig. 4, we observe that both iterative receivers significantly outperform the conventional single-user receiver. When a

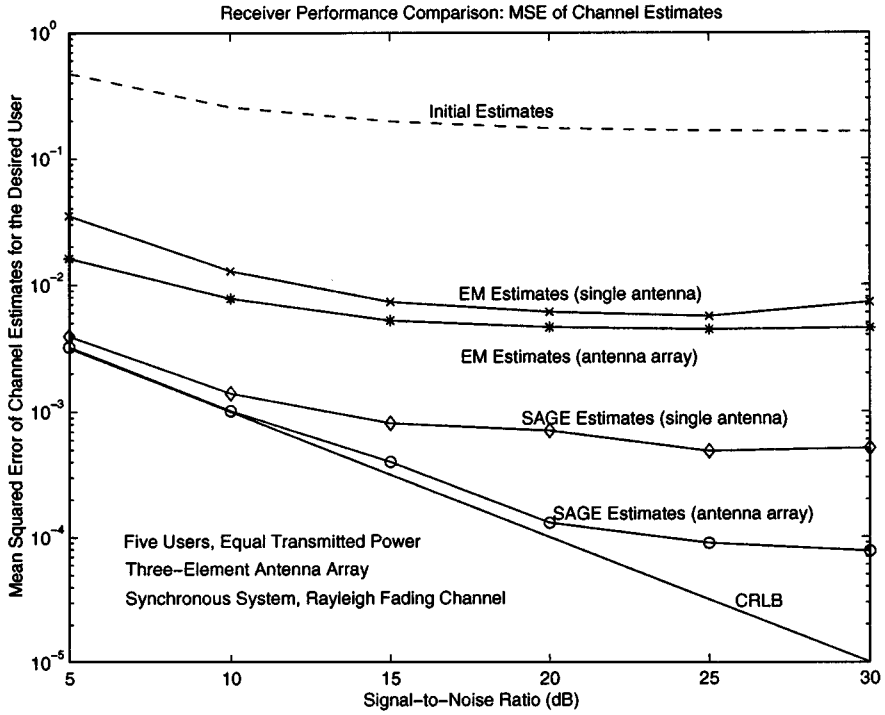

Fig. 5. Mean squared error of channel estimates for single antenna and a three-element antenna array.

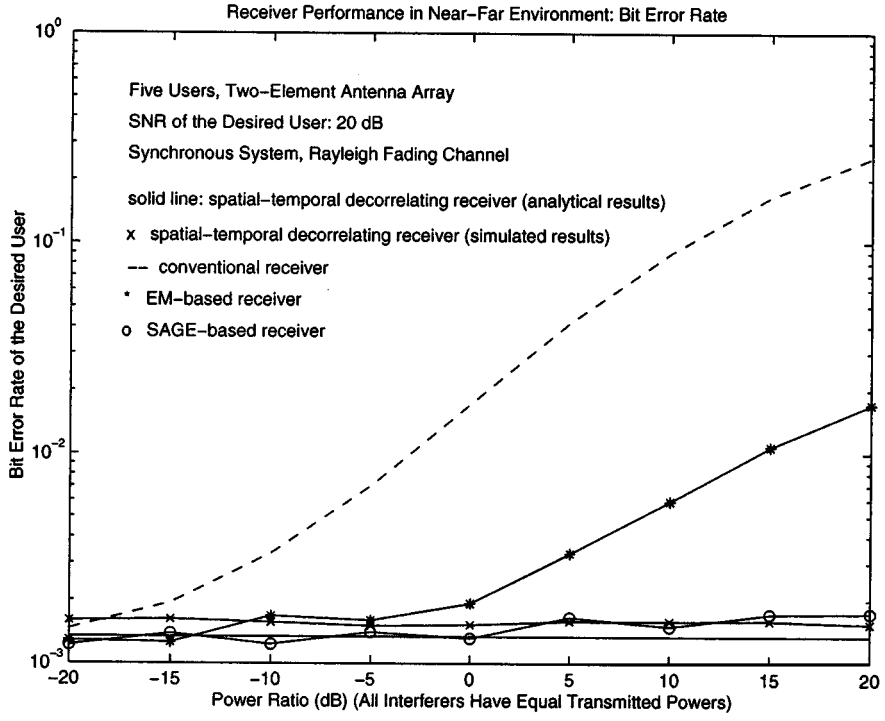

Fig. 6. BER for a two-element antenna array in a near–far environment.

single antenna is used, however, the iterative receivers do not converge to the optimal spatial-temporal decorrelating receiver. However, the SAGE-based receiver performance is greatly enhanced using an antenna array. This is mainly due to improved channel estimation by the antenna array, as shown in Fig. 5. When the SNR is larger than 20 dB, the channel estimates of the SAGE-based receiver do not reach the CRLB. However, the loss in channel estimation performance at such a high SNR does not have a strong effect on symbol detection. At a BER of 10^{-2}, a three-element antenna array can achieve about 6-dB gain over a single antenna.

To assess near–far resistance, we consider five active users and a two-element antenna array. We assume that the first user is the desired user with 20-dB SNR and fixed

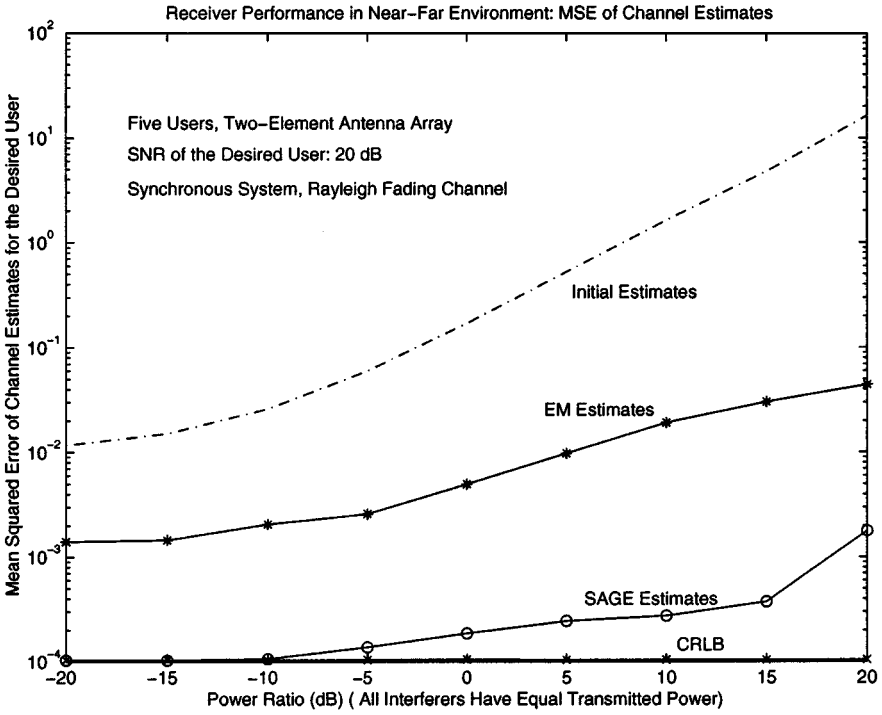

Fig. 7. Mean squared error of channel estimates for a two-element antenna array in near–far environment.

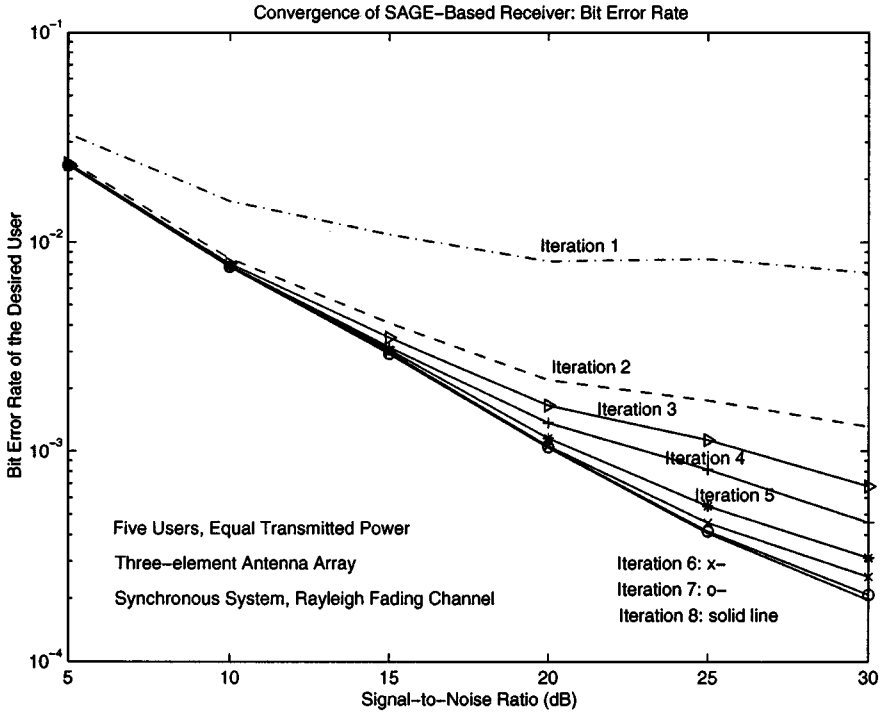

Fig. 8. Convergence of SAGE-based receiver for a three-element antenna array.

transmitted power. All other interferers are assumed to have equal and varying transmitted power, and eight iterations are used. At 20-dB power ratio, transmitted powers of the interferers are all 100 times stronger than that of the desired user and represents an extreme near–far environment. Over these many other experiments, we have observed that the SAGE-based receiver achieves good near–far performance by the third iteration [28]. Fig. 6 shows that the SAGE-based receiver outperforms the EM-based receiver, converges to the spatial-temporal decorrelating receiver with perfect array channel knowledge and exhibits near–far resistance. As depicted in Fig. 7, neither the EM-based receiver nor the conventional single-user receiver exhibits near–far resistance.

Fig. 8 illustrates convergence of the SAGE-based receiver iterations. Five users with equal transmitted power are used along with a three-element base-station antenna-array. We note that

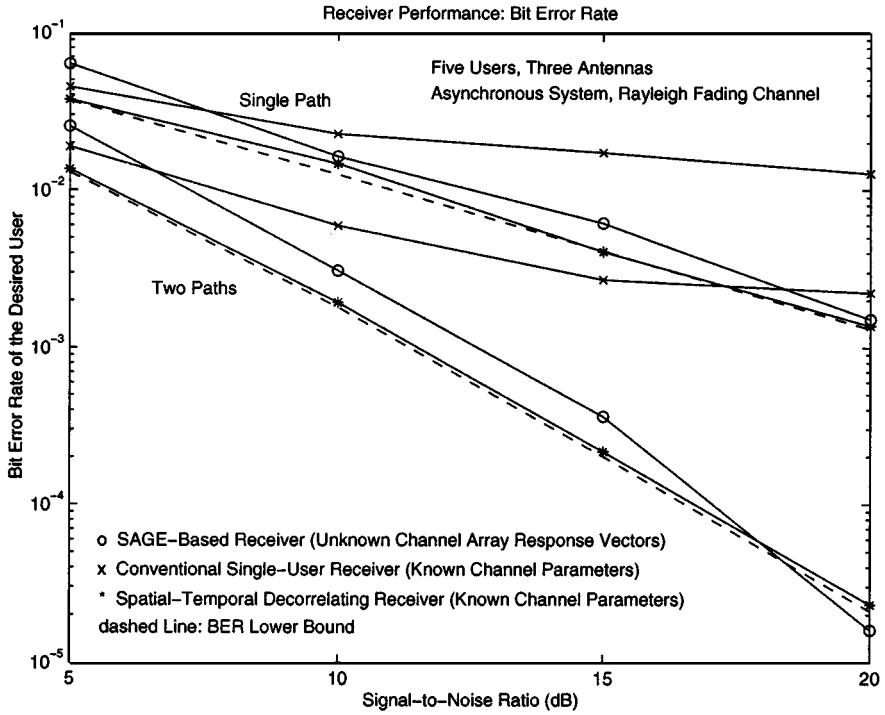

Fig. 9. Receiver performance in multipath fading. Dashed lines represent the BER lower bounds (48) applied to one and two-path channels.

the SAGE-based receiver converges very quickly in the low SNR region, and that most of the gain can be realized in three to four iterations.

Fig. 9 compares BER performance for a two-path Rayleigh fading channel where time delays of the first and second paths for each user are uniformly distributed in $(0, T_b/2)$ and $(T_b/2, T_b)$, respectively. Identical temporal covariance matrices are assumed for all paths. The channel array response vectors are assumed to be known for both the spatial-temporal decorrelating and conventional single-user receivers. A three-element antenna array is used at the base-station and all users have equal transmitted power. As expected, maximal-ratio RAKE combining of the two paths can achieve significant BER performance gain over that of a receiver locked onto the dominant path. Although the BER performance of the conventional single-user receiver for two-path channels outperforms that for single-path channels, both exhibit a BER floor due to multiple-access interference. As shown, the SAGE-based multiuser receiver achieves improved performance, while the approximate BER lower bound predicts ideal spatial-temporal decorrelator performance.

VII. Conclusion

We have derived an uplink spatial-temporal decorrelator for an antenna array-equipped CDMA basestation. The new decorrelator exhibits near–far resistance. Numerical results show that the incorporation of an antenna array results in significant improvement in performance and convergence in a fading channel. An iterative receiver structure is developed via the SAGE algorithm, and the BER and CRLB are derived. Performance gains are shown to be significant over a conventional single-user receiver. The SAGE-based receiver outperforms an EM-based receiver and approaches the BER of the spatial-temporal decorrelating receiver. The channel estimates of the SAGE-based receiver are also close to the CRLB. The simulated BER agrees closely with analytical results.

References

[1] R. Lupas and S. Verdu, "Near–far resistance of multiuser detectors in asynchronous channels," *IEEE Trans. Commun.*, vol. 38, pp. 496–508, Apr. 1990.

[2] S. Verdu, "Minimum probability of error for asynchronous Gaussian multiple-access channels," *IEEE Trans. Inform. Theory*, vol. IT-32, pp. 85–96, Jan. 1986.

[3] Z. Xie, R. T. Short, and C. K. Rushforth, "A family of suboptimum detectors for coherent multiuser communications," *IEEE J. Select. Areas Commun.*, vol. 8, pp. 683–690, May 1990.

[4] M. K. Varanasi and B. Aazhang, "Multistage detection in asynchronous code-division multiple-access communications," *IEEE Trans. Commun.*, vol. 38, pp. 509–519, Apr. 1990.

[5] A. Duel-Hallen, "Decorrelating decision-feedback multiuser detector for synchronous code-division multiple-access channel," *IEEE Trans. Commun.*, vol. 41, pp. 285–290, Feb. 1993.

[6] Z. Zvonar and D. Brady, "Multiuser detection in single-path fading channels," *IEEE Trans. Commun.*, vol. 42, pp. 1729–1739, Feb./Mar./Apr. 1994.

[7] A. J. Paulraj and C. B. Papadias, "Space-time processing for wireless communications," *IEEE Signal Processing Mag.*, pp. 49–83, Nov. 1997.

[8] A. F. Naguib and A. Paulraj, "Performance of wireless CDMA with M-ary orthogonal modulation and cell site antenna arrays," *IEEE J. Select. Areas Commun.*, vol. 14, pp. 1770–1783, May 1996.

[9] H. Liu and M. D. Zoltowski, "Blind equalization in antenna array CDMA systems," *IEEE Trans. Signal Processing*, vol. 45, pp. 161–172, Jan. 1997.

[10] R. Kohno, H. Imai, M. Hatori, and S. Pasupathy, "Combination of an adaptive array antenna and a canceller of interference for direct-sequence spread-spectrum multiple-access system," *IEEE J. Select. Areas Commun.*, vol. 8, pp. 675–681, May 1990.

[11] S. Y. Miller and S. C. Schwartz, "Integrated spatial-temporal detectors for asynchronous Gaussian multiple-access channels," *IEEE Trans. Commun.*, vol. 43, pp. 396–411, Feb./Mar./Apr. 1995.

[12] M. Feder and E. Weinstein, "Parameter estimation of superimposed signals using the EM algorithm," *IEEE Trans. Acoust., Speech, Signal Processing*, vol. 36, pp. 477–489, Apr. 1988.
[13] C. N. Georghiades and J. C. Han, "Sequence estimation in the presence of random parameters via the EM algorithm," *IEEE Trans. Commun.*, vol. 45, pp. 300–308, Mar. 1997.
[14] L. B. Nelson and H. V. Poor, "Iterative multiuser receivers for CDMA channels: An EM-based approach," *IEEE Trans. Commun.*, vol. 44, pp. 1700–1710, Dec. 1996.
[15] U. Fawer and B. Aazhang, "A multiuser receiver for code division multiple access communications over multipath channels," *IEEE Trans. Commun.*, vol. 43, pp. 1556–1565, Feb./Mar./Apr. 1995.
[16] R. Wang and S. D. Blostein, "Spatial-temporal CDMA receiver structures for rayleigh fading channels," in *Proc. Int. Conf. Communications (ICC)*, Vancouver, BC, Canada, June 1999, pp. S15.3.1–S15.3.5.
[17] J. A. Fessler and A. O. Hero, "Space-alternating generalized EM algorithm," *IEEE Trans. Signal Processing*, vol. 42, pp. 2664–2677, Oct. 1994.
[18] D. Dahlhaus, A. Jarosch, B. H. Fleury, and R. Heddergott, "Joint demodulation in DS/CDMA systems exploiting the space and time diversity of the mobile radio channel," in *Proc. IEEE Int. Symp. Personal, Indoor and Mobile Radio Communications*, Helsinki, Finland, 1997, pp. 47–52.
[19] I. Sharfer and A. O. Hero, "Optimum multiuser CDMA detector using grouped coordinate ascent and the DWT," in *Proc. IEEE Workshop in Signal Processing Advances in Wireless Communications*, Paris, France, Apr. 1997.
[20] A. Duel-Hallen, J. Holtzman, and Z. Zvonar, "Multiuser detection for CDMA systems," *IEEE Pers. Commun.*, pp. 46–58, Apr. 1995.
[21] U. Madhow, "Blind adaptive interference suppression for the near–far resistant acquisition and demodulation of direct-sequence CDMA signals," *IEEE Trans. Signal Processing*, vol. 45, pp. 124–136, Jan. 1997.
[22] R. Lupas and S. Verdu, "Linear multiuser detectors for synchronous code-division multiple-access channels," *IEEE Trans. Inform. Theory*, vol. 35, pp. 123–136, Jan. 1989.
[23] C. F. J. Wu, "On the convergence properties of the EM algorithm," *Ann. Statist.*, vol. 11, no. 1, pp. 95–103, Jan. 1983.
[24] A. O. Hero and J. A. Fessler, "Convergence in norm for alternating expectation-maximization (EM) type algorithms," *Statistica Sinica*, vol. 5, no. 1, pp. 41–54, Jan. 1995.
[25] A. M. Monk, M. Davis, and L. B. Milstein, "A noise-whitening approach to multiple access noise rejection—Part I: Theory and background," *IEEE J. Select. Areas Commun.*, vol. 12, pp. 817–827, June 1994.
[26] J. G. Proakis, *Digital Communications*, 3rd ed. New York: McGraw-Hill, 1995.
[27] P. Stoica and A. Nehorai, "Music, maximum likelihood, and Cramer-Rao bound," *IEEE Trans. Acoust., Speech, Signal Processing*, vol. 37, pp. 720–741, May 1989.
[28] R. Wang, "Spatial-Temporal Signal Processing for Multi-User CDMA Communication Systems," Ph.D. dissertation, Queen's Univ., Kingston, ON, Canada, 1999.

Ruifeng Wang (S'96–M'00) received the B.S. and M.S. degrees from Northern Jiaotong University, Beijing, China, in 1986 and 1989, respectively, and the Ph.D. degree from Queen's University, Kingston, ON, Canada, in 1999, all in electrical engineering.

Before joining Queen's University as a Ph.D. student and Research Assistant in 1995, he was a Hardware Design Engineer at The Sixth Research Institute, Ministry of Electronics Industry, Beijing, China. From 1999 to 2000, he was with the research and development department, COM DEV, Cambridge, ON, Canada. He is currently with AT&T Wireless Local Technologies Group, Redmond, WA. His research interests lie in statistical signal processing and wireless communications.

Steven D. Blostein (S'83–M'88–SM'96) received the B.S. degree in electrical engineering from Cornell University, Ithaca, NY, in 1983, and the M.S. and Ph.D. degrees in electrical and computer engineering from the University of Illinois, Urbana-Champaign, in 1985 and 1988, respectively.

He has been on the Faculty at Queen's University, Kingston, ON, Candad, since 1988 and currently holds the position of Associate Professor in the Department of Electrical and Computer Engineering. He has been a consultant to both industry and government in the areas of document image compression, motion estimation, and target tracking, and was a Visiting Associate Professor in the Department of Electrical Engineering, McGill University, in 1995. His current interests lie in statistical signal processing, wireless communications, and video image communications.

Dr. Blostein served as Chair of IEEE Kingston Section (1993–1994) and Associate Editor for IEEE TRANSACTIONS ON IMAGE PROCESSING (1996–2000). He currently leads the Multirate Wireless Data Access Major Project sponsored by the Canadian Institute for Telecommunications Research. He is a registered Professional Engineer in Ontario.